Published in final edited form as:
Dev Biol. 2011 July 15; 355(2): 215–226. doi:10.1016/j.ydbio.2011.04.021.

Pinpointing the Expression of piRNAs and Function of the PIWI Protein Subfamily during Spermatogenesis in the Mouse

Ergin Beyret[1,2] and **Haifan Lin**[2,*]

[1]Department of Cell Biology, Duke University Medical School, Durham, NC 27710

[2]Yale Stem Cell Center and Department of Cell Biology, Yale University School of Medicine, New Haven, CT 06509

SUMMARY

PIWI proteins and piRNAs have been linked to transposon silencing in the primordial mouse testis, but their function in the adult testis remains elusive. Here we report the cytological characterization of piRNAs in the adult mouse testis and the phenotypic analysis of *Miwi*$^{-/-}$; *Mili*$^{-/-}$ mice. We show that piRNAs are specifically present in germ cells, especially abundant in spermatocytes and early round spermatids, regardless of the type of the genomic sequences to which they correspond. piRNAs and PIWI proteins are present in both the cytoplasm and nucleus. In the cytoplasm, they are enriched in the chromatoid body; whereas in the nucleus they are enriched in the dense body, a male-specific organelle associated with synapsis and the formation of the XY body during meiosis. Moreover, by generating *Miwi*$^{-/-}$; *Mili*$^{-/-}$ mice, which lack all PIWI proteins in the adult, we show that PIWI proteins and presumably piRNAs in the adult are required only for spermatogenesis. Spermatocytes without PIWI proteins are arrested at the pachytene stage, when the sex chromosomes undergo transcriptional silencing to form the XY body. These results pinpoint a function of the PIWI protein subfamily to meiosis during spermatogenesis.

Keywords

PIWI; piRNA; sex chromosome; chromatoid body; spermatogenesis; meiosis

INTRODUCTION

All sexually reproducing organisms undergo meiosis to decrease their genomic content by half for reproduction. A central aspect of meiosis is the pairing of the homologous chromosomes, which has to be under strict regulation since any mis-pairing can lead to aneuploidy in the progeny. However, unpaired regions naturally occur in the male mice as a consequence of the heteromorphic sex chromosomes unlike the females, whose morphologically identical sex chromosomes can fully synapse, just like the autosomes. Consequently, the sex chromosomes in the male are recognized and sequestered as the heterochromatinized structure “XY body” during meiosis (Hoyer-Fender, 2003).

*Corresponding Author: Haifan.lin@yale.edu (phone: 203-785-6239; fax 203-785-4305).

The XY body is discerned during pachynema and diplonema as a darkly stained globular chromatin structure, and marked by the phosphorylation of the H2A variant H2AX (γH2AX) (Hoyer-Fender, 2003). It is formed *en route* to the transcriptional inactivation of the sex chromosomes as a manifestation of meiotic silencing of unpaired chromosomes (MSUC) (Baarends et al., 2005; Turner, 2007; Turner et al., 2006; Turner et al., 2005). MSUC, in turn, is thought to be a protective mechanism against aneuploidy since the transcriptional silencing of a chromosome is likely to render a germ cell unviable. This phenomenon is similar to the RNAi-related meiotic silencing by unpaired DNA (MSUD) in *Neurospora crassa*, whereby unpaired sequences are recognized and silenced in conjunction with homologous sequences in-trans as a means to protect the genome from retrotransposon invasion during mating (Huynh and Lee, 2003; Kelly and Aramayo, 2007; Shiu et al., 2001)

As the catalytic components of the RNAi machinery, PIWI/ARGONAUTE protein family is a highly conserved group of proteins present in prokaryotes and eukaryotes (Cerutti and Casas-Mollano, 2006; Hall, 2005). It was first discovered with the identification of *piwi* in *Drosophila* during a mutational screen for the genes affecting germline stem cell maintenance (Cox et al., 1998; Lin and Spradling, 1997). Phylogenetic analysis of this protein family deciphers the divergence of two sub-families, called ARGONAUTE (*AGO*) and PIWI, based on their resemblance to *Arabidopsis thaliana* AGO1 and *Drosophila melanogaster* PIWI. Of these two groups, AGO proteins have been shown to regulate gene expression via miRNAs and siRNAs, whereas the function of PIWI proteins is still relatively elusive (Peters and Meister, 2007).

In pursuit of the functional characterization of PIWI proteins, we and others independently discovered a unique class of non-coding small RNAs in mammalian testes, which are named PIWI-interacting RNAs (piRNAs) due to their interaction with PIWI proteins (Aravin et al., 2006; Girard et al., 2006; Grivna et al., 2006; Lau et al., 2006; Watanabe et al., 2006). The size of piRNAs varies depending on the particular interacting PIWI homolog, and ranges mostly between 24–32nt. Furthermore, PIWI proteins are necessary for their expression and/or stability. Subsequent works identified piRNAs in various organisms that express PIWI proteins, including protists (Mochizuki et al., 2002; Mochizuki and Gorovsky, 2004), insects (Yin and Lin, 2007), worms (Batista et al., 2008), fishes (Houwing et al., 2008), and amphibians (Wilczynska et al., 2009). PIWI proteins and piRNAs are found predominantly in the gonads of the animals or exclusively during the sexual reproductive cycle of the protists (Mochizuki et al., 2002). Echoing this expression pattern, mutations in animal PIWI proteins all result in infertility due to defects in germline determination and gametogenesis (Harris and Macdonald, 2001; Klattenhoff and Theurkauf, 2008; Megosh et al., 2006). Therefore, PIWI proteins and presumably their partnering piRNAs in the animals have an essential function for germ cells.

The mouse genome consists of three PIWI homologs: MIWI, MILI, and MIWI2 (Peters and Meister, 2007). They are all abundantly expressed in the male germline (Aravin et al., 2008; Deng and Lin, 2002; Kuramochi-Miyagawa et al., 2001; Kuramochi-Miyagawa et al., 2008; Unhavaithaya et al., 2008). Among these, only MILI and its associated piRNAs have also been detected in the female germline (Aravin et al., 2008; Kuramochi-Miyagawa et al., 2008). However, loss of MILI, MIWI, or MIWI2 causes only spermatogenic arrest with no oogenic or maternally derived defects. While knocking out *Miwi* causes post-meiotic arrest of spermatogenesis, *Mili*$^{-/-}$ or *Miwi2*$^{-/-}$ mice show spermatogenic arrest between early and mid-pachytene stage of meiosis with prior defects in stem cell maintenance and self-renewal (Carmell et al., 2007; Deng and Lin, 2002; Kuramochi-Miyagawa et al., 2004; Unhavaithaya et al., 2008). Since PIWI proteins are necessary for the biogenesis and/or stability of piRNAs, oocytes in the *Mili*$^{-/-}$ mouse are expected to be devoid of MILI-associated

piRNAs as well. These observations implicate that murine PIWI/piRNA complexes predominantly function in spermatogenesis.

A likely molecular activity of murine PIWI-piRNA complexes in spermatogenesis is transposon silencing as most *piwi* mutations in various organisms cause increased transposition of certain types of transposons (Aravin et al., 2007; Carmell et al., 2007; Chambeyron et al., 2008; Das et al., 2008; Desset et al., 2008; Houwing et al., 2008; Sarot et al., 2004; Vagin et al., 2006). Moreover, most piRNA sequences in *Drosophila* match transposons (Brennecke et al., 2007; Yin and Lin, 2007) and the downregulation of the piRNAs is correlated with the increased activity of the corresponding types of transposons (Brennecke, Aravin et al. 2007). Similarly, in the primordial mouse testis, MILI and MIWI2 associate with piRNAs rich in transposonic sequences, as compared to piRNAs in the adult testis (Aravin et al., 2008; Kuramochi-Miyagawa et al., 2008). In the absence of MILI or MIWI2 , Line1 and IAP type transposons are hypomethylated, and their mRNA levels are upregulated specifically in the germline (Aravin et al., 2007; Carmell et al., 2007; Kuramochi-Miyagawa et al., 2008). Therefore, it has been proposed that PIWI proteins use piRNAs to target and silence transposons in the germline.

Although the primordial mouse testis contains abundant piRNAs with transposonic sequences, adult testicular piRNAs are mostly derived from non-transposonic regions (Aravin et al., 2006; Aravin et al., 2007; Girard et al., 2006). Therefore, the majority of piRNAs in the adult testis seems to function independently of transposon regulation. To elucidate this function, here we report the phenotypic and cytological characterization of PIWI proteins and piRNAs in the adult mouse testis. We show that both PIWI proteins and piRNAs are specifically found in germ cells, where they are present in both the nucleus and cytoplasm. They are enriched in the male germ-cell specific structures the chromatoid body and the dense body. Moreover, piRNAs are highly up-regulated in the meiotic cells regardless of the type of the genomic regions they correspond to. In the $Miwi^{-/-};Mili^{-/-}$ adult testis where none of the three PIWI proteins is detectable, spermatogenesis is arrested during pachynema, when the sex chromosomes undergo transcriptional inactivation. These results indicate an essential function of PIWI proteins and piRNAs in male meiosis.

MATERIALS AND METHODS

Animals

The generation and genetic backgrounds of $Mili^{-/-}$ and $Miwi^{-/-}$ mice have been previously described by Deng *et al* and Kuramochi-Miyagawa *et al* (2004), respectively. The homozygous mutants were obtained by crossing heterozygous males to homozygous mutant females. CD1 strain mice were used as the wild type control and in the identification of the piRNAs associated with MILI and MIWI.

Denaturing PAGE analysis of piRNAs

Indicated amount of RNA samples were denatured in 50% formamide at 55C° for 15 minutes. The samples were resolved in a polyacrylamide gel containing 6M Urea with 1X TBE. Radiolabeled samples were analyzed by exposure to X-ray films (Kodak) or phosphorimager screens.

Small RNA Northern blotting

Following denaturing PAGE, the gel was stained with 1μg/ml ethidium bromide in 1X TBE for ~15 minutes to assess the global piRNA content and integrity of the samples. Afterwards, the gel was de-stained in 1X TBE for ~10 minutes and transferred onto Hybond-N™ nylon membrane (Amersham Biosciences) in 1X TBE for 30 minutes at

350miliAmp using a Hoefer TE 22 tank transfer unit at 4C°. The membrane was dried at 75C° for 5–10 minutes. The samples were cross-linked to the membrane with UV light of 120mJ/cm^2 followed by baking at 75C° for one hour. The membrane was either stored at −80C° until needed or used immediately for probing. Hybridization was performed overnight at 42C° in [5X SSC, 20mM Na_2HPO_4 at pH 7.2, 7% SDS, 1X Denhardt`s Solution, 0.1mg/ml boiled salmon sperm DNA] following prehybridization in the same buffer composition without Denhardt's Solution for at least 30 minutes at 42C°. Probes were prepared as follows: DNA oligonucleotides with reverse complementary sequences for individual small RNAs were obtained from IDT, Inc. and radiolabeled on their 5` ends with kinase reaction. For piRNAs, oligos were LNA-modified to yield a Tm value of 75C° (+/−3C°). Labeled probes were boiled for 1 minute before adding into the hybridization buffer. Following hybridization, blots were washed twice in 1×SSC and 0.1% SDS at 42°C for 10 minutes and analyzed by PhosphorImager. If necessary, blots were stripped by boiling in 0.1% SDS for 10 minutes.

Antibodies

The following antibodies were used for indirect immunofluorescence at the indicated dilution: R133 anti-MIWI 1:200 (Deng and Lin, 2002), GP15 anti-MILI 1:200 (Unhavaithaya et al., 2008), anti-SCP1 1:25 (Santa Cruz), anti-SCP3 1:50 (Novus Biologicals) anti-EE2 1:200, anti-CyclinD3 1:100, anti-CREM-I (X-12) 1:200 (Santa Cruz Biotechnology), anti-H3K9me2 1:400 (Cell Signaling), anti-H3K9me3 1:250 (Abcam), anti-TRA54 1:400, anti-Tsx 1:1000, anti-Fibrillarin 1:300 (Novus Biologicals), anti-γH2AX 2–5μg/ml (Millipore), anti-acetyl-Histone H4 (Lys16) 1:200 (Millipore), anti-PolII (S5) (Bethyl Lab) 1:100, anti-BC7 1:100. Fluorophore-conjugated secondary antibodies obtained from Jackson Immuno Research Laboratories were used between 1:100–1:1000. Dilution factors for immunoblotting: anti-GAPDH 1:4000 (Sigma), anti-Pol II (CTD4H8) 1:1000 (Santa Cruz Biotechnology), R133 anti-MIWI 1:1000, GP15 anti-MILI 1:1500, MILI peptide antibody 1:1500 (Unhavaithaya et al., 2008). HRP-conjugated secondary antibodies obtained from Jackson Immuno Research Laboratories were used between 1:1000–1:10000.

Spermatocyte spread preparation

Mice at indicated ages were euthanized with cervical dislocation or asphyxiation with CO_2. The testicular cells were mechanically isolated as previously described (Aravindan et al., 1996) from flash-frozen testes with the following modifications: The 1X PBS solution used until the fixation of the samples was kept ice-cold and supplemented with [complete mini EDTA-free Protease inhibitor cocktail tablet (Roche), 1mM EDTA, 1mM DTT]. The cell suspension was filtered sequentially through 70μm and 20μm nylon mesh, and lastly through glass wool that were equilibrated with 1X PBS pre- and post-filtration. The cells were precipitated at 700g for 10 minutes at 4C° and resuspended in 100μl of the hypotonic extraction buffer of (Peters et al., 1997) per testicular sample. Nuclei were spread as in (Peters et al., 1997) with the following modifications: The samples were precipitated at 700g for 10 minutes at 4C° after the incubation in the hypotonic solution. The pellet was resuspended in 50μl of the 1X PBS solution and supplemented with 50μl 100mM sucrose (pH8.2) per testicular sample. 20μl of the suspension was spread per slide. Spread nuclei were dried in a humidifying chamber at 55C° for 2 hours before washing with the Photoflo (Kodak) solution. The slides were dried at room temperature and kept at −80C° until needed.

Immunofluorescence analyses

Unless otherwise indicated, 8–10μm cyrosections were used. Freshly dissected whole testes were fixed in [4% paraformaldehyde-1X PBS] solution overnight at 4C°. The next day, they were dehydrated by sequential incubation in 10-15–20-30% sucrose solutions in 1X PBS at room temperature for 30-45–60-60 minutes respectively, followed by [30% sucrose-1X

PBS] : OCT (1:1) overnight at 4C° and [30% sucrose-1X PBS] : OCT (1:3) for 30 to 60 minutes at room temperature. The samples were cryopreserved in OCT at −80C° until sectioning.

For immunoflourescence detection of proteins on cryosections, samples were first re-hydrated with 1X PBS and then incubated in the blocking solution of 10% serum in 1X PBT [1X PBS, 0.1% BSA, 0.1% Tween-20] for at least one hour at room temperature. Afterwards, samples were sequentially treated with the primary and secondary antibodies diluted in the same blocking solution. Incubations with the antibodies were performed at room temperature for 2 hours or at 4C° overnight. Following the secondary antibody treatment, the samples were stained with DAPI in 1X PBT for 6 minutes at room temperature to visualize the DNA. The samples were rinsed with 1X PBT for three times 10 minutes each, following the primary antibody incubation, and once again after DAPI staining. Slides were mounted with VectaShield mounting medium (Vector Labs).

In situ detection of piRNAs

LNA-modified DNA oligonucleotides with reverse complementary sequences of individual piRNAs were labeled with the DIG Oligonucleotide Tailing Kit (Roche) according to the manufacturer's instructions and purified with Sephadex G25 Columns. Labeling efficiency was estimated by dot blotting based on the reference set provided by the kit. The hybridization buffer is composed of [50% (v:v) deionised formamide, 0.3M NaCl, 20mM Tris HCl pH8.0, 5mM EDTA, 10mM $NaPO_4$ buffer pH8.0, 10% (w:v) Dextran Sulfate, 1X Denhardt's Solution, 100μg/ml PolyA oligo DNA of 30nt length, 0.1 mg/ml Heparin and freshly boiled 0.5 mg/ml yeast tRNA]. Before the hybridization, the sections were acetylated with freshly made [0.25% acetic anhydride, 1.165% triethanolamine] for 10 minutes followed by 1X PBS wash for three times five minutes each. Probes were incubated in the hybridization buffer at 65C° for 5 minutes and quickly chilled on ice to denature secondary structures. Hybridization was performed overnight at 46C° in a humidifying chamber of [1XSSC, 50% formamide] after sealing the slides with a hybrislip. Following the hybridization, the slides were washed for 15 minutes once with 5X SSC at room temperature, twice with [50% formamide, 0.1% Tween-20, 1X SSC] at 46C°,, once with 0.5X SSC at room temperature, and finally once with1X PBS at room temperature. Antibody detection was performed as in (Heller et al., 1998) except the concentration of the alkaline-phosphatase (AP) conjugated F_{ab} fragments (Boehringer Mannheim) used was 1:750, and PBS in the last two washes were replaced with NTL buffer [150mM NaCl, 100mM Tris-HCl pH8.1, 0.5mg/ml Levamisole]. The slides were incubated in the dark with 1-STEP NBT/BCIP plus Suppressor Solution (Pierce) until the desired color intensity was reached. Color development was terminated with [1X PBS pH 5.5, 1mM EDTA].

Combined RNA and protein detection was performed similar to RNA detection alone with the following modifications in the antibody detection: Primary antibodies for the counter staining were combined with the AP conjugated F_{ab} fragments. Following the incubation, the slides were washed three times at room temperature in 1X PBT for 15 minutes each. The samples were incubated with a combination of the secondary antibodies and AP-conjugated F_{ab} fragments in the same blocking buffer for 2 hours at room temperature or overnight at 4C°. Washes were performed as in RNA detection alone. The slides were additionally washed with [0.1M Tris-HCl pH 8.1, 0.5mg/ml Levamisole] for 15 minutes then incubated in the dark with FastRed solution (Roche). [1X PBS pH 5.5, 1mM EDTA] was used to terminate the color development.

In situ detection of Cot-1 RNA

Spermatocyte spreads from an 18dpp *Miwi*$^{+/-}$;*Mili*$^{+/-}$ mouse were prepared as indicated above under RNase-free conditions and kept at −80C°. Before the hybridization, they were washed at room temperature once with [0.5% Triton X-100, 1X PBS] for 5 minutes, once with [4% paraformaldehyde-1X PBS] for 10 minutes, and three times with 1X PBS for 5 minutes each. Afterwards, they were acetylated as in *in situ* detection of piRNAs, and dehydrated with a stepwise wash at room temperature with 70%, 90% and 100% ethanol, respectively for 2 minutes each that was repeated twice at each step. The slides were dried for 3 minutes at room temperature before the hybridization with the probe. The probe was prepared from 1μg mouse Cot-1 DNA (Invitrogen) per sample as previously reported (Zhang et al., 2009) except it was labeled with Fluor-12-dUTP provided with the Prime-It Fluor fluorescence labeling kit (Stratagene), resuspended in 10μl 1X TE after the ethanol precipitation and kept in dark at −20C°. For the hybridization, it was mixed with 40μl of the same hybridization buffer used for the *in situ* detection of piRNAs, except the yeast tRNA was excluded. The hybridization mixture was boiled for 5 minutes and chilled on ice before adding onto the spermatocyte spread samples. Hybridization reaction and post-hybridization washes were performed as in *in situ* detection of piRNAs except the hybridization temperature was kept at 42C° and the slides were washed with the [50% formamide, 0.1% Tween-20, 1X SSC] solution at 45C°. phospho-PolII S5 and γH2AX were stained following the post-hybridization washes in the same way as indicated in the immunoflourescence detection of proteins.

Probes used for *in situ* hybridization and Northern blotting

The nucleotides with the "+" sign on their left are LNA-modified.

mir-34b	: CAA +TC+A G+CT +AA+T TA+C A+CT +GC+C TA
mir-100	: C+AA +GTT +CG+G AT+C TA+C G+GG +TT
mir-465	: T+CA +CA+T C+AG +TG+C C+AT +TC+T AAA +TA
mir-16	: CGC CAA TAT TTA CGT GCT GCT A
Negative Oligo	: AA+C GA+C TCG CAG TA+C GTC A+CG T+CT A+TG G
U6 snRNA	: TGT GCT GCC GAA GCG AGC AC

piRNA probes:

Sense Intronic 2 and piRNA T4 are MIWI piRNAs, the rest are MILI-associated.

Transposonic 1	: G+AG +CC+G C+CC +TCA CAT TCG CTG TTG CA
Transposonic 2	: GGA C+CG +GT+C T+GC AG+C TGC TGA GTC GTA
Sense Exonic	: GGG CTC TGT GGT +GG+C T+TT +TCG TCG TGC CA
Anti-sense Exonic	: GGG ACA CA+C T+CA +GC+A C+TC +CT+T TGC A
Sense Intronic 1	: GGG CAG GTG +AG+A G+GA +TCC ATG GCC CA
Sense Intronic 2	: TAG G+CC +CTT +CAT +CA+C G+GA +TG+G ATT ATT GAG
Anti-sense Intronic	: GAA CCA GTT C+CA +CG+A G+TG +TT+G C+CC A
Repeat-associated 1	: TA+T CA+T A+GT +CA+T CA+T CA+T C+AT +CG+T CA
Repeat-associated 2	: G+TA +GGT +CT+C CAG CA+T CA+C A+TC T+TT G+TA
piRNA T4	: TAG ACA ATT TTC AGT GTC CTA AGC TGT CTA

Chromosome painting

X and Y chromosomes were painted on spermatocyte spreads with the probes obtained from Cambio (StarFISH Mouse Chromosome Specific Probes) according to the manufacturer's recommendations except: Spermatocyte spreads were washed at room temperature once in

0.5% TritonX-100 for 5 minutes and three times in 1X PBS for 2 minutes each before incubating in methanol:acetic acid (3:1) for 10 minutes. Denaturation of the probes and the slides were performed at 70C° for 2 minutes. The probes and the prepared slides were introduced at 65C° and the temperature was gradually decreased to 37C°, at which it was kept overnight for the hybridization. γH2AX staining was performed as above in between the hybridization and the detection steps following the post-hybridization washes. The slides were mounted with VectaShield mounting medium (Vector Labs) after counter-staining with DAPI. Images were analyzed with Axioimager (Carl Zeiss Incorporation). 3D images were captured using Apotome deconvolution microscopy.

Separation of the nuclear and cytoplasmic fractions of the testicular lysate

A pair of two-month-old adult testes, which had been flash-frozen and stored at −80C°, was homogenized with a tight (B) pestle (clearance: 0.0010–0.0030 inch, Kontes Glass Company) in 1ml of the same lysis buffer used for immunoprecipitation. The lysate was spun at 1300g for 10 minutes at 4C° to precipitate the nuclei and intact cells. The supernatant was spun one more time to remove residual nuclei and kept as the “cytoplasmic fraction”. The pellet was washed with 500μl lysis buffer, grinded again to eliminate contaminating unbroken cells and respun. After one more round of cleaning, the pellet was lastly resuspended in 1 ml lysis buffer and kept as the “nuclear fraction”. The supernatants of the washes were pooled and kept as the “wash fraction”. For the unfractionated control, a pair of testes was likewise homogenized in 1 ml buffer without any further separation. Total RNAs were extracted from equal volumes of the samples, fractionated with 15% Urea-PAGE and northern blotted to assess their piRNA content. 25 μg kidney total RNA was used as a negative control for piRNAs. The blot was stripped and re-probed with a 30mer LNA-modified oligo DNA with no matching sequence on the genome as a negative control for hybridization (*Data not shown*). Likewise, equal volumes were analyzed with western blotting onto nitrocellulose membranes (Bio-Rad Laboratories) to assess their MILI-MIWI content and the degree of cross contamination.

RESULTS

Testicular piRNAs are germline-specific and highly abundant in spermatocytes

We and others have previously shown that piRNAs overall are highly up-regulated by 22dpp, when spermiogenesis is initiated, but are not detectable in the adult epididymide, where mature sperm are stored (Aravin et al., 2006; Girard et al., 2006; Grivna et al., 2006; Watanabe et al., 2006). These observations indicate that piRNAs have a significant function during spermatogenesis and are not paternally loaded to the embryo. To further explore their spermatogenic function, we analyzed the expression profiles of individual piRNAs during postnatal testicular development with Northern blotting. We chose representative piRNAs derived from different types of sequences in the genome, including repeat-associated and transposonic regions, to test if they have different expression patterns. Irrespective of their genomic annotation, all of the four tested piRNAs become highly abundant by 22dpp, but are not detectable before 14dpp by northern blotting (Figure 1). This period corresponds to the first wave of meiosis. Thus, piRNAs are up-regulated during meiosis, just like their protein partners MILI and MIWI (Deng and Lin, 2002; Kuramochi-Miyagawa et al., 2004; Kuramochi-Miyagawa et al., 2001; Unhavaithaya et al., 2008), implying a potential function of PIWI/piRNA complexes during meiosis irrespective of their genomic origins.

To further characterize piRNA expression during meiosis, we performed *in situ* hybridization of representative piRNAs on the adult testis. We first assessed if our technique is reliable in the detection of small RNAs by comparing the Northern and *in situ* expression profiles of several micro RNAs (miRNAs) during spermatogenesis. As expected, a miRNA

with a decreasing Northern expression profile during spermatogenesis was enriched in the early spermatogenetic cells in our *in situ* analysis; whereas those with an increasing expression profile were enriched accordingly later in the germ cells (Supplementary Figure 1). These data validate our small RNA *in situ* analysis technique.

We then conducted *in situ* hybridization for a total of 17 piRNAs, four of which are MIWI-associated and the rest are MILI-associated. We chose these piRNAs based on their corresponding genomic origin, including repeat-associated, transposonic, exonic and intronic regions. All of these piRNAs are up-regulated during the mid-stages of spermatogenesis (Figure 2), agreeing with the Northern data. Particularly, piRNAs are strongly expressed in spermatocytes and also present in round spermatids. In addition, some probes yielded signal in the basal layer of the tubule where spermatogonia reside. This expression pattern is consistent with the expression patterns of MILI and MIWI (Aravin et al., 2008; Deng and Lin, 2002; Grivna et al., 2006; Kuramochi-Miyagawa et al., 2004; Unhavaithaya et al., 2008; Wang et al., 2009).

Even though different piRNAs with similar sequences may associate with both MILI and MIWI, we noticed the same pattern of staining in *Miwi*$^{-/-}$ testis as well (data not shown), where MILI piRNAs, but not MIWI piRNAs, are detected (Beyret, 2009). These results indicate that MILI piRNAs exist both in spermatocytes and round spermatids, in addition to spermatogonia (Beyret, 2009) and primordial germ cells (Aravin et al., 2008; Kuramochi-Miyagawa et al., 2008). Unfortunately we cannot conduct the same test for MIWI piRNAs since the germline does not progress beyond the mid-pachynema in *Mili*$^{-/-}$ testis (Kuramochi-Miyagawa et al., 2004).

In order to more precisely identify the expression window of piRNAs during spermatogenesis, we co-stained adult testis for piRNAs and cell-specific markers. This analysis showed that piRNA expression is close to the background level in spermatogonia, highly elevated in spermatocytes, moderate in round spermatids and already decreases to an undetectable level by the time elongating spermatids are formed (Figure 3).

We also analyzed if piRNA expression in the mouse testis is germline-specific, since this is the case for PIWI proteins (Aravin et al., 2008; Deng and Lin, 2002; Kuramochi-Miyagawa et al., 2004; Kuramochi-Miyagawa et al., 2001; Unhavaithaya et al., 2008). The mouse testis consists of three types of resident somatic cells: Sertoli cells are the only somatic cell types inside the seminiferous tubules, Myeoid and Leydig cells reside in the interstitial space. We noticed that the piRNAs tested are not detectable in these cell types (Figure 3). Therefore, piRNAs in the mouse testis appear to be germline-specific, just like their partners PIWI proteins.

piRNAs localize to the nuage/chromatoid body in the cytoplasm and the dense body in the nucleus of spermatogenic cells

To further characterize the spatial expression pattern of piRNAs, we examined their subcellular localization. piRNAs mainly localize to the cytoplasm of the germ cells, including perinuclear granules that are likely nuage/chromatoid body (Figure 2 C–D), where PIWI proteins have also been shown to be enriched; (Aravin et al., 2008; Batista et al., 2008; Beyret, 2009; Grivna et al., 2006; Houwing et al., 2007; Kotaja et al., 2006; Malone et al., 2009; Unhavaithaya et al., 2008; Wang et al., 2009). This highly dynamic germline-specific structure has been proposed to act as a warehouse and processing center for RNAs produced during early spermatogenesis to be used later (Kotaja et al., 2006; Kotaja and Sassone-Corsi, 2007; Parvinen, 2005; Soderstrom and Parvinen, 1976) and as a surveillance checkpoint to monitor the trafficking of transposon intermediates through nuclear pores via the piRNA pathway (Aravin et al., 2008; Klattenhoff and Theurkauf, 2008).

In addition, piRNAs are detected in the nuclei of early spermatocytes, where they localize to a punctum of approximately 1–2 micrometer in each nucleus (Figure 2 G). To explore the potential function of piRNAs in the nucleus, we characterized this nuclear structure by immunofluorescence. MIWI and MILI largely co-localize with piRNAs in spermatocytes, including at this punctum (Figure 4 A–G). This punctum is unlikely a background staining, because our antibodies are highly specific (Supplementary Figure 2). Moreover, it does not correspond to the piRNA-encoding genomic sequence, because it is devoid of DNA (Figure 4 H–I). It is not nucleolus or Cajal body either, as indicated by the lack of fibrillarin, a common marker for these structures (Figure 4 H–K). These properties of the punctum are consistent with those of the dense body, a male-specific electro-dense structure of 1–2μm diameter found in early spermatocyte nuclei only (Dresser and Moses, 1980; Fletcher, 1979; Goetz et al., 1984; Moses, 1977; Takanari et al., 1982). Although the function of the dense body is elusive, it has been observed to interact with the sex chromosomes (Dresser and Moses, 1980; Fletcher, 1979; Moses, 1977). In correlation, subsequently in round spermatids, we noticed that MILI localizes to the peri-chromocenter (Figure 4 L–M), and this sub-nuclear domain has been shown to correspond to the sex chromosomes (Turner et al., 2006).

We next asked if the nuclear and cytosolic staining in our *in situ* analyses indeed represent piRNAs rather than a precursor or complementary transcript. For this purpose, we separated adult testicular extract into nuclear and cytoplasmic fractions and analyzed for their piRNA content with ethidium bromide staining and Northern blotting. This analysis revealed that, irrespective of their genomic origin, a substantial amount of piRNAs as well as MIWI and MILI does exist in the nucleus in addition to the cytoplasm (Figure 5).

Spermatogenesis is arrested during pachynema in the absence of PIWI proteins

Since a component of the dense body has been shown to be necessary for the proper synapsis and the formation of the XY body (Crackower et al., 2003; Kolas et al., 2005), we analyzed if any of these events is impaired in the absence of PIWI proteins by conducting chromosome painting on *Miwi*$^{-/-}$; *Mili*$^{-/-}$ spermatocyte spreads. The reason we used the *Miwi*$^{-/-}$; *Mili*$^{-/-}$ double mutant is that MIWI and MILI, but not MIWI2, are expressed in meiosis I prophase (Deng and Lin, 2002; Kuramochi-Miyagawa et al., 2004; Kuramochi-Miyagawa et al., 2008; Unhavaithaya et al., 2008). In addition, MILI is necessary for the assembly and localization of the MIWI2/piRNA complex in the primordial testis (Aravin et al., 2008). In the absence of MILI, MIWI2 is largely mis-localized and MIWI2 piRNAs are not detected. Hence, *Miwi*$^{-/-}$; *Mili*$^{-/-}$ mice are expected to be as defective as *Miwi*$^{-/-}$; *Mili*$^{-/-}$; *Miwi2*$^{-/-}$ mice. Furthermore, the *Miwi*$^{-/-}$; *Mili*$^{-/-}$ double mutant phenocopies the *Mili*$^{-/-}$ (Kuramochi-Miyagawa et al., 2004) and *Miwi2*$^{-/-}$ (Carmell et al., 2007) mutants but not the *Miwi*$^{-/-}$ mutant (Deng and Lin, 2002) (Figure 6 and Supplementary Figure 3). Thus, the double mutant represents the loss-of-function of all three PIWI/piRNA complexes in the mouse.

We observed that X and Y chromosomes in *Miwi*$^{-/-}$; *Mili*$^{-/-}$ spermatocytes are in the vicinity of each other and covered with globular γH2AX staining (Figure 7A–D). In addition to marking double stranded breaks (Mahadevaiah et al., 2001; Rogakou et al., 1998), γH2AX also marks any unpaired region during meiosis (Mahadevaiah et al., 2001; Turner, 2007). It coats the sex chromosomes of the late zygotene spermatocytes in a tadpole-like shape during the zygonema-pachynema transition and takes the globular form of the XY body during pachynema (Blanco-Rodriguez, 2009; Mahadevaiah et al., 2001). Therefore, our results indicate that homolog recognition as well as formation of the XY body is not impaired. Co-staining for the axial/lateral element SCP3 and the transverse element SCP1 of the synaptonemal complex did not indicate any overall obvious defect in synapsis among the several examples examined, even though we noticed that SCP1 staining was somewhat faint

in *Miwi*$^{-/-}$; *Mili*$^{-/-}$ spermatocytes (Figure 7E–J). These results indicate that the spermatogenic arrest occurs during mid-pachynema and PIWI proteins are not required for the pairing of the homologous chromosomes or in sequestering the sex chromosomes for the formation of the XY body.

Since the time point of the spermatogenic arrest coincides with transcriptional silencing of the sex chromosomes, we first examined the epigenetic status of the XY body in *Miwi*$^{-/-}$; *Mili*$^{-/-}$ spermatocytes. Due to its highly heterochromatinized nature, the XY body is normally rich in heterochromatin marks and lacks euchromatin marks. For instance, the heterochromatin marks H3K9me2 and H3K9me3 abundantly accumulate in the XY body between early and late pachynema (Khalil et al., 2004; van der Heijden et al., 2007). We observed that sex chromosomes in *Miwi*$^{-/-}$*; Mili*$^{-/-}$ spermatocytes all remain hypomethylated for H3K9me2. However, in depth comparison with the relative stage control spermatocytes indicated that this effect appears to be due to the spermatogenic arrest occurring before the hypermethylation. (Figure 8 A–H). Similarly, we did not detect any significant difference in the pattern of H3K9me3 coating over the XY body (Supplementary Figure 4).

In addition, we examined for an earlier epigenetic mark, acetyl-H4K16, which marks euchromatin and disappears from the sex chromosomes upon formation of the XY body during early pachynema (Khalil et al., 2004). Interestingly, we observed that, in most of the early *Miwi*$^{-/-}$; *Mili*$^{-/-}$ pachytene spermatocytes, XY bodies are still covered with the mark, which becomes undetectable only in mid-pachytene spermatocytes (Figure 8 I–O). Thus, this modification appears to be retarded to mid-pachynema in *Miwi*$^{-/-}$; *Mili*$^{-/-}$ spermatocytes.

To determine whether these cells escape meiotic silencing of the sex chromosomes, we stained them for Serine-5-phosphorylated RNA polymerase II (phospho-PolII S5), which marks the initiation of transcription. We found that, similar to the control samples (Figure 9 A–C), phospho-PolII S5 signal gradually disappears from the XY bodies of *Miwi*$^{-/-}$; *Mili*$^{-/-}$ spermatocytes (Figure 9 D–F) as they progress through pachynema. The lack of phospho-PolII S5 signal on the XY body is recapitulated by the lack of Cot-1 RNA, which represents the nascent transcripts (Figure 9G–I) (Hall et al., 2002; Huynh and Lee, 2003; Zhang et al., 2009). These observations indicate that the sex chromosomes in *Miwi*$^{-/-}$; *Mili*$^{-/-}$ spermatocytes can still undergo transcriptional silencing.

DISCUSSIONS

Here we have characterized the function of murine PIWI proteins and piRNAs during spermatogenesis by phenotypic analyses of *Miwi*$^{-/-}$*;Mili*$^{-/-}$ mice and cytological analyses of piRNAs and the two PIWI proteins. Because these mice lack all the PIWI proteins in the adult testes, our results indicate that PIWI proteins are indispensable for only meiosis due to the spermatogenic arrest during pachynema. We also show that piRNAs in the mouse testis are germ cell-specific with abundant expression in spermatocytes and early round spermatids. Additionally, we show that piRNAs are found in the cytoplasm as well as in the nucleus, where they co-localize with the PIWI proteins MILI and MIWI. In the cytoplasm, piRNAs localize to the nuage/chromatoid body in addition to the homogenous cytosolic distribution; whereas in the nucleus, MILI, MIWI and piRNAs are enriched in the dense body, a male-specific sub-nuclear structure found exclusively in spermatocytes during prophase I of meiosis. Interestingly, in the absence of PIWI proteins, spermatogenesis is terminally arrested during this period.

Our finding that piRNAs are germ cell-specific and highly up-regulated during meiosis in synchrony with PIWI proteins suggests that PIWI-piRNA complexes have a significant function during meiosis. Indeed, *Miwi*$^{-/-}$; *Mili*$^{-/-}$ adult mice, which lack all PIWI proteins, display complete spermatogenic arrest during meiosis, phenocopying *Mili*$^{-/-}$ mice. We did not observe any other phenotype including embryonic, somatic, oogenic or maternally derived defects. Because PIWI proteins partner with piRNAs which depend on PIWI proteins for their expression/stability, and MIWI2 piRNAs are not detectable in the absence of MILI (Aravin et al., 2008), *Miwi*$^{-/-}$; *Mili*$^{-/-}$ mice are devoid of all piRNAs. Therefore, our results indicate that murine piRNAs as well as PIWI proteins are indispensable only for the progression of spermatogenesis and particularly during meiosis. Although maintenance and division of the spermatogonial stem cells and their progenitors are impaired in the *Mili*$^{-/-}$ mice (Unhavaithaya et al., 2008), currently it is not clear whether these phenotypes represent an independent stem cell function of MILI or whether they are merely an indirect effect of the spermatogenic arrest during meiosis.

What is the male-specific meiotic function of PIWI proteins and piRNAs? Although PIWI proteins and piRNAs have been implicated in the silencing of the transposons in the premeiotic germline (Aravin et al., 2008; Kuramochi-Miyagawa et al., 2008), piRNAs with transposonic sequences (a.k.a rasiRNAs) constitute only a minor fraction of the adult testicular piRNAs, which is enriched with meiotic piRNAs (Aravin et al., 2006; Girard et al., 2006). This observation indicates that the majority of piRNAs in the adult can not function in targeting transposons. Indeed, we did not observe any difference in the expression patterns of the piRNAs that differed according to their genomic origin. Instead, the colocalization of PIWI proteins and piRNAs to two male-specific structures, the chromatoid body and the dense body, indicates that PIWI proteins and piRNAs might achieve their male-specific functions through these two structures.

The chromatoid body is believed to be the manifestation of the nuage in spermatocytes and spermatids. Although the nuage is a fibrous material surrounding the nucleus and specific to germ cells, the chromatoid body is a peri-nuclear sphere observed in only spermatocytes and round spermatids. It is thought to be an RNA processing and storage center (Kotaja et al., 2006; Kotaja and Sassone-Corsi, 2007; Parvinen, 2005; Soderstrom and Parvinen, 1976), and also an intra and inter-cellular carrier vessel (Ventela et al., 2003). Thus, the chromatoid body may be the site of piRNA production from the precursors and/or functions in shuttling piRNAs to their destinations.

Our study also shed light onto the function of the dense body. The dense body has been described in the Chinese hamster spermatocytes (Dresser and Moses, 1980; Moses, 1977; Takanari et al., 1982) as well as in the mouse (Fletcher, 1979; Goetz et al., 1984) as a dynamic structure during prophase I of meiosis. In the mouse, it is detectable from pachynema until diplonema and can be found away from the XY body before mid-pachynema but associates with the distally unpaired portion of the X chromosome during mid-to-late pachynema (Dresser and Moses, 1980; Fletcher, 1979; Moses, 1977). Its appearance and subsequent association with the sex chromosomes during male meiosis is suggestive of its involvement in the modification and/or behavior of the sex chromosomes in the male during meiosis and possibly afterwards. Until now, only one protein, FKBP6, has been shown to be a component of the dense body in the mouse (Crackower et al., 2003; Kolas et al., 2005). Mice that lack FKBP6 only display male-specific infertility due to spermatogenic arrest during pachynema, and show defects in synapsis (Crackower et al., 2003) and the formation of the XY body (Kolas et al., 2005). Here we show that, the PIWI proteins MILI and MIWI, as well as their piRNAs, also localize to the dense body, adding new components to this elusive structure.

We did not detect any defect in the homolog recognition and synapsis of the chromosomes, or in the formation of the XY body in *Miwi*$^{-/-}$; *Mili*$^{-/-}$ mice. This observation is different from the phenotype of the *Fkbp6*$^{-/-}$ mice, implicating a different function of PIWI proteins in pachynema. Additionally, the sex chromosomes in *Miwi*$^{-/-}$; *Mili*$^{-/-}$ spermatocytes still undergo meiotic silencing. Thus, PIWI proteins and piRNAs must be involved in the other aspects of meiosis. Because MILI is also localized to peri-chromocenter in round spermatids, where the sex chromosomes localize, it is possible that MILI and, presumably, piRNAs are involved in functions related to sex chromosomes, such as in paternal imprinting of the X chromosome.

What makes the PIWI proteins indispensable for meiosis? Although we did not detect any significant defect in the silencing of the sex chromosomes in *Miwi*$^{-/-}$;*Mili*$^{-/-}$ spermatocytes, it is still possible that the PIWI/piRNA complexes may function in meiotic silencing and/or epigenetic modification due to the strong evidence in other systems where small RNA pathways are involved in similar mechanisms (Kelly and Aramayo, 2007; Lee et al., 2003; Mochizuki et al., 2002; Mochizuki and Gorovsky, 2004; She et al., 2009; Shiu et al., 2001). In addition there is strong evidence for the epigenetic involvement of PIWI in Drosophila (Yin and Lin, 2007). Another possible function of the PIWI proteins is their involvement in the crossing-over process during meiosis. This possibility is supported by our observation that the spermatogenic arrest in *Miwi*$^{-/-}$;*Mili*$^{-/-}$ mice corresponds to the time point when crossing-over takes place. Interestingly, a DNA helicase involved in DNA repair and recombination, is a component of a piRNA complex in the rat testis (Lau et al., 2006). Systematic comparison of the epigenetic status and recombination activities of the chromatin during spermatogenesis in wildtype versus the *piwi* mutants should shed light on these issues.

Supplementary Material

Refer to Web version on PubMed Central for supplementary material.

Acknowledgments

We thank Dr. Yoshitake Nishimune for the EE2, TRA54 and BC7 antibodies; Dr. Debra J. Wolgemuth for the Cyclin D3 antibody; Dr. Philip Avner for the Tsx antibody; and Yi Hao for nuclear immunostaining of MILI in round spermatids. We are grateful to Hua Li, Thihan Padukkavidana, Jason Hanna and Danielle Martin for their assistance in piRNA *in situ* analysis. We also thank Na Liu, Katherine Uyhazi, Nicole Darricarrere, Xiao Huang and Li Liu for their valuable comments on this manuscript. This work is supported by National Institutes of Health Grants HD42012, the G. Harold and Leila Mathers Foundation, the Connecticut Stem Cell Research Fund (06SCD01, 06SCE01, and 08SCD-Yale-004), and the G. Harold and Leila Mathers Foundation.

REFERENCES

Aravin A, et al. A novel class of small RNAs bind to MILI protein in mouse testes. Nature. 2006; 442:203–207. [PubMed: 16751777]

Aravin AA, et al. A piRNA pathway primed by individual transposons is linked to de novo DNA methylation in mice. Mol Cell. 2008; 31:785–799. [PubMed: 18922463]

Aravin AA, et al. Developmentally regulated piRNA clusters implicate MILI in transposon control. Science. 2007; 316:744–747. [PubMed: 17446352]

Aravindan GR, et al. Ability of trypsin in mimicking germ cell factors that affect Sertoli cell secretory function. J Cell Physiol. 1996; 168:123–133. [PubMed: 8647906]

Baarends WM, et al. Silencing of unpaired chromatin and histone H2A ubiquitination in mammalian meiosis. Mol Cell Biol. 2005; 25:1041–1053. [PubMed: 15657431]

Batista PJ, et al. PRG-1 and 21U-RNAs interact to form the piRNA complex required for fertility in C. elegans. Mol Cell. 2008; 31:67–78. [PubMed: 18571452]

Beyret, E. Cell Biology. Vol. Vol. Durham: Ph.D. Duke University; 2009. Function of the Mouse PIWI Proteins and Biogenesis of Their piRNAs in the Male Germline.

Blanco-Rodriguez J. gammaH2AX marks the main events of the spermatogenic process. Microsc Res Tech. 2009

Brennecke J, et al. Discrete small RNA-generating loci as master regulators of transposon activity in Drosophila. Cell. 2007; 128:1089–1103. [PubMed: 17346786]

Carmell MA, et al. MIWI2 is essential for spermatogenesis and repression of transposons in the mouse male germline. Dev Cell. 2007; 12:503–514. [PubMed: 17395546]

Cerutti H, Casas-Mollano JA. On the origin and functions of RNA-mediated silencing: from protists to man. Curr Genet. 2006; 50:81–99. [PubMed: 16691418]

Chambeyron S, et al. piRNA-mediated nuclear accumulation of retrotransposon transcripts in the Drosophila female germline. Proc Natl Acad Sci U S A. 2008; 105:14964–14969. [PubMed: 18809914]

Cox DN, et al. A novel class of evolutionarily conserved genes defined by piwi are essential for stem cell self-renewal. Genes Dev. 1998; 12:3715–3727. [PubMed: 9851978]

Crackower MA, et al. Essential role of Fkbp6 in male fertility and homologous chromosome pairing in meiosis. Science. 2003; 300:1291–1295. [PubMed: 12764197]

Das PP, et al. Piwi and piRNAs act upstream of an endogenous siRNA pathway to suppress Tc3 transposon mobility in the Caenorhabditis elegans germline. Mol Cell. 2008; 31:79–90. [PubMed: 18571451]

Deng W, Lin H. miwi, a murine homolog of piwi, encodes a cytoplasmic protein essential for spermatogenesis. Dev Cell. 2002; 2:819–830. [PubMed: 12062093]

Desset S, et al. In Drosophila melanogaster the COM locus directs the somatic silencing of two retrotransposons through both Piwi-dependent and -independent pathways. PLoS ONE. 2008; 3:e1526. [PubMed: 18253480]

Dresser ME, Moses MJ. Synaptonemal complex karyotyping in spermatocytes of the Chinese hamster (Cricetulus griseus). IV. Light and electron microscopy of synapsis and nucleolar development by silver staining. Chromosoma. 1980; 76:1–22. [PubMed: 6153596]

Fletcher JM. Light microscope analysis of meiotic prophase chromosomes by silver staining. Chromosoma. 1979; 72:241–248. [PubMed: 88315]

Girard A, et al. A germline-specific class of small RNAs binds mammalian Piwi proteins. Nature. 2006; 442:199–202. [PubMed: 16751776]

Goetz P, et al. Morphological and temporal sequence of meiotic prophase development at puberty in the male mouse. J Cell Sci. 1984; 65:249–263. [PubMed: 6538881]

Grivna ST, et al. A novel class of small RNAs in mouse spermatogenic cells. Genes Dev. 2006; 20:1709–1714. [PubMed: 16766680]

Hall LL, et al. An ectopic human XIST gene can induce chromosome inactivation in postdifferentiation human HT-1080 cells. Proc Natl Acad Sci U S A. 2002; 99:8677–8682. [PubMed: 12072569]

Hall TM. Structure and function of argonaute proteins. Structure. 2005; 13:1403–1408. [PubMed: 16216572]

Harris AN, Macdonald PM. Aubergine encodes a Drosophila polar granule component required for pole cell formation and related to eIF2C. Development. 2001; 128:2823–2832. [PubMed: 11526087]

Heller S, et al. Molecular markers for cell types of the inner ear and candidate genes for hearing disorders. Proc Natl Acad Sci U S A. 1998; 95:11400–11405. [PubMed: 9736748]

Houwing S, et al. Zili is required for germ cell differentiation and meiosis in zebrafish. Embo J. 2008; 27:2702–2711. [PubMed: 18833190]

Houwing S, et al. A role for Piwi and piRNAs in germ cell maintenance and transposon silencing in Zebrafish. Cell. 2007; 129:69–82. [PubMed: 17418787]

Hoyer-Fender S. Molecular aspects of XY body formation. Cytogenet Genome Res. 2003; 103:245–255. [PubMed: 15051945]

Huynh KD, Lee JT. Inheritance of a pre-inactivated paternal X chromosome in early mouse embryos. Nature. 2003; 426:857–862. [PubMed: 14661031]

Kelly WG, Aramayo R. Meiotic silencing and the epigenetics of sex. Chromosome Res. 2007; 15:633–651. [PubMed: 17674151]

Khalil AM, et al. Dynamic histone modifications mark sex chromosome inactivation and reactivation during mammalian spermatogenesis. Proc Natl Acad Sci U S A. 2004; 101:16583–16587. [PubMed: 15536132]

Klattenhoff C, Theurkauf W. Biogenesis and germline functions of piRNAs. Development. 2008; 135:3–9. [PubMed: 18032451]

Kolas NK, et al. Mutant meiotic chromosome core components in mice can cause apparent sexual dimorphic endpoints at prophase or X-Y defective male-specific sterility. Chromosoma. 2005; 114:92–102. [PubMed: 15983832]

Kotaja N, et al. The chromatoid body of male germ cells: similarity with processing bodies and presence of Dicer and microRNA pathway components. Proc Natl Acad Sci U S A. 2006; 103:2647–2652. [PubMed: 16477042]

Kotaja N, Sassone-Corsi P. The chromatoid body: a germ-cell-specific RNA-processing centre. Nat Rev Mol Cell Biol. 2007; 8:85–90. [PubMed: 17183363]

Kuramochi-Miyagawa S, et al. Mili, a mammalian member of piwi family gene, is essential for spermatogenesis. Development. 2004; 131:839–849. [PubMed: 14736746]

Kuramochi-Miyagawa S, et al. Two mouse piwi-related genes: miwi and mili. Mech Dev. 2001; 108:121–133. [PubMed: 11578866]

Kuramochi-Miyagawa S, et al. DNA methylation of retrotransposon genes is regulated by Piwi family members MILI and MIWI2 in murine fetal testes. Genes Dev. 2008; 22:908–917. [PubMed: 18381894]

Lau NC, et al. Characterization of the piRNA complex from rat testes. Science. 2006; 313:363–367. [PubMed: 16778019]

Lee DW, et al. An argonaute-like protein is required for meiotic silencing. Genetics. 2003; 164:821–828. [PubMed: 12807800]

Lin H, Spradling AC. A novel group of pumilio mutations affects the asymmetric division of germline stem cells in the Drosophila ovary. Development. 1997; 124:2463–2476. [PubMed: 9199372]

Mahadevaiah SK, et al. Recombinational DNA double-strand breaks in mice precede synapsis. Nat Genet. 2001; 27:271–276. [PubMed: 11242108]

Malone CD, et al. Specialized piRNA pathways act in germline and somatic tissues of the Drosophila ovary. Cell. 2009; 137:522–535. [PubMed: 19395010]

Megosh HB, et al. The role of PIWI and the miRNA machinery in Drosophila germline determination. Curr Biol. 2006; 16:1884–1894. [PubMed: 16949822]

Mochizuki K, et al. Analysis of a piwi-related gene implicates small RNAs in genome rearrangement in tetrahymena. Cell. 2002; 110:689–699. [PubMed: 12297043]

Mochizuki K, Gorovsky MA. Conjugation-specific small RNAs in Tetrahymena have predicted properties of scan (scn) RNAs involved in genome rearrangement. Genes Dev. 2004; 18:2068–2073. [PubMed: 15314029]

Moses MJ. Synaptonemal complex karyotyping in spermatocytes of the Chinese hamster (Cricetulus griseus). II. Morphology of the XY pair in spread preparations. Chromosoma. 1977; 60:127–137. [PubMed: 870291]

Parvinen M. The chromatoid body in spermatogenesis. Int J Androl. 2005; 28:189–201. [PubMed: 16048630]

Peters AH, et al. A drying-down technique for the spreading of mammalian meiocytes from the male and female germline. Chromosome Res. 1997; 5:66–68. [PubMed: 9088645]

Peters L, Meister G. Argonaute proteins: mediators of RNA silencing. Mol Cell. 2007; 26:611–623. [PubMed: 17560368]

Rogakou EP, et al. DNA double-stranded breaks induce histone H2AX phosphorylation on serine 139. J Biol Chem. 1998; 273:5858–5868. [PubMed: 9488723]

Sarot E, et al. Evidence for a piwi-dependent RNA silencing of the gypsy endogenous retrovirus by the Drosophila melanogaster flamenco gene. Genetics. 2004; 166:1313–1321. [PubMed: 15082550]

She X, et al. Regulation of heterochromatin assembly on unpaired chromosomes during Caenorhabditis elegans meiosis by components of a small RNA-mediated pathway. PLoS Genet. 2009; 5:e1000624. [PubMed: 19714217]

Shiu PK, et al. Meiotic silencing by unpaired DNA. Cell. 2001; 107:905–916. [PubMed: 11779466]

Soderstrom KO, Parvinen M. Incorporation of (3H)uridine by the chromatoid body during rat spermatogenesis. J Cell Biol. 1976; 70:239–246. [PubMed: 932099]

Takanari H, et al. Dense bodies in silver-stained spermatocytes of the Chinese hamster: behavior and cytochemical nature. Chromosoma. 1982; 86:359–373. [PubMed: 6217037]

Turner JM. Meiotic sex chromosome inactivation. Development. 2007; 134:1823–1831. [PubMed: 17329371]

Turner JM, et al. Pachytene asynapsis drives meiotic sex chromosome inactivation and leads to substantial postmeiotic repression in spermatids. Dev Cell. 2006; 10:521–529. [PubMed: 16580996]

Turner JM, et al. Silencing of unsynapsed meiotic chromosomes in the mouse. Nat Genet. 2005; 37:41–47. [PubMed: 15580272]

Unhavaithaya Y, et al. MILI, a piRNA binding protein, is required for germline stem cell self-renewal and appears to positively regulate translation. J Biol Chem. 2008

Vagin VV, et al. A distinct small RNA pathway silences selfish genetic elements in the germline. Science. 2006; 313:320–324. [PubMed: 16809489]

van der Heijden GW, et al. Chromosome-wide nucleosome replacement and H3.3 incorporation during mammalian meiotic sex chromosome inactivation. Nat Genet. 2007; 39:251–258. [PubMed: 17237782]

Ventela S, et al. Intercellular organelle traffic through cytoplasmic bridges in early spermatids of the rat: mechanisms of haploid gene product sharing. Mol Biol Cell. 2003; 14:2768–2780. [PubMed: 12857863]

Wang J, et al. Mili interacts with tudor domain-containing protein 1 in regulating spermatogenesis. Curr Biol. 2009; 19:640–644. [PubMed: 19345100]

Watanabe T, et al. Identification and characterization of two novel classes of small RNAs in the mouse germline: retrotransposon-derived siRNAs in oocytes and germline small RNAs in testes. Genes Dev. 2006; 20:1732–1743. [PubMed: 16766679]

Wilczynska A, et al. Two Piwi proteins, Xiwi and Xili, are expressed in the Xenopus female germline. Rna. 2009; 15:337–345. [PubMed: 19144913]

Yin H, Lin H. An epigenetic activation role of Piwi and a Piwi-associated piRNA in Drosophila melanogaster. Nature. 2007; 450:304–308. [PubMed: 17952056]

Zhang LF, et al. Telomeric RNAs mark sex chromosomes in stem cells. Genetics. 2009; 182:685–698. [PubMed: 19380904]

Highlights

- piRNAs are specifically present in germ cells, especially in spermatocytes.
- piRNAs and PIWI proteins are present in both the cytoplasm and nucleus.
- In the cytoplasm, they are enriched in the chromatoid body;
- In the nucleus, they are enriched in the dense body.
- Spermatocytes without PIWI proteins are arrested at the pachytene stage.

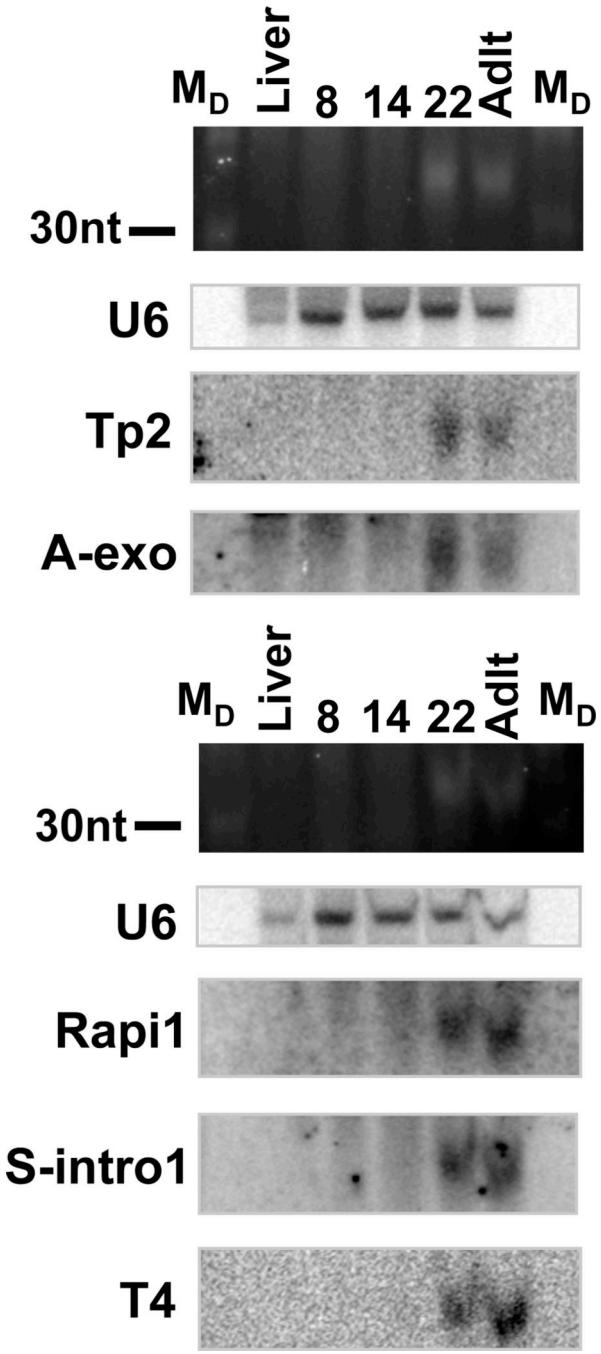

Figure 1. piRNAs become abundant during meiosis

Northern blotting analysis of individual piRNAs shows that piRNAs are up-regulated during meiosis irrespective of their genomic origin. Each panel corresponds to an individual piRNA with a different origin (e.g., sense intronic: a piRNA derived from the sense strand of an intron). 20μg of total RNA from 8dpp, 14dpp, 22dpp and two-month-old adult wild type testes was analyzed. 20μg of liver total RNA was used as a negative control for piRNAs. U6 snRNA (U6) was used as an internal loading control. M_D: 10nt DNA marker, Tp2: Transposonic 2, A-exo: Anti-sense exonic, Rapi1: Repeat-associated 1, S-Intro1: Sense intronic 1, T4: piRNA-T4.

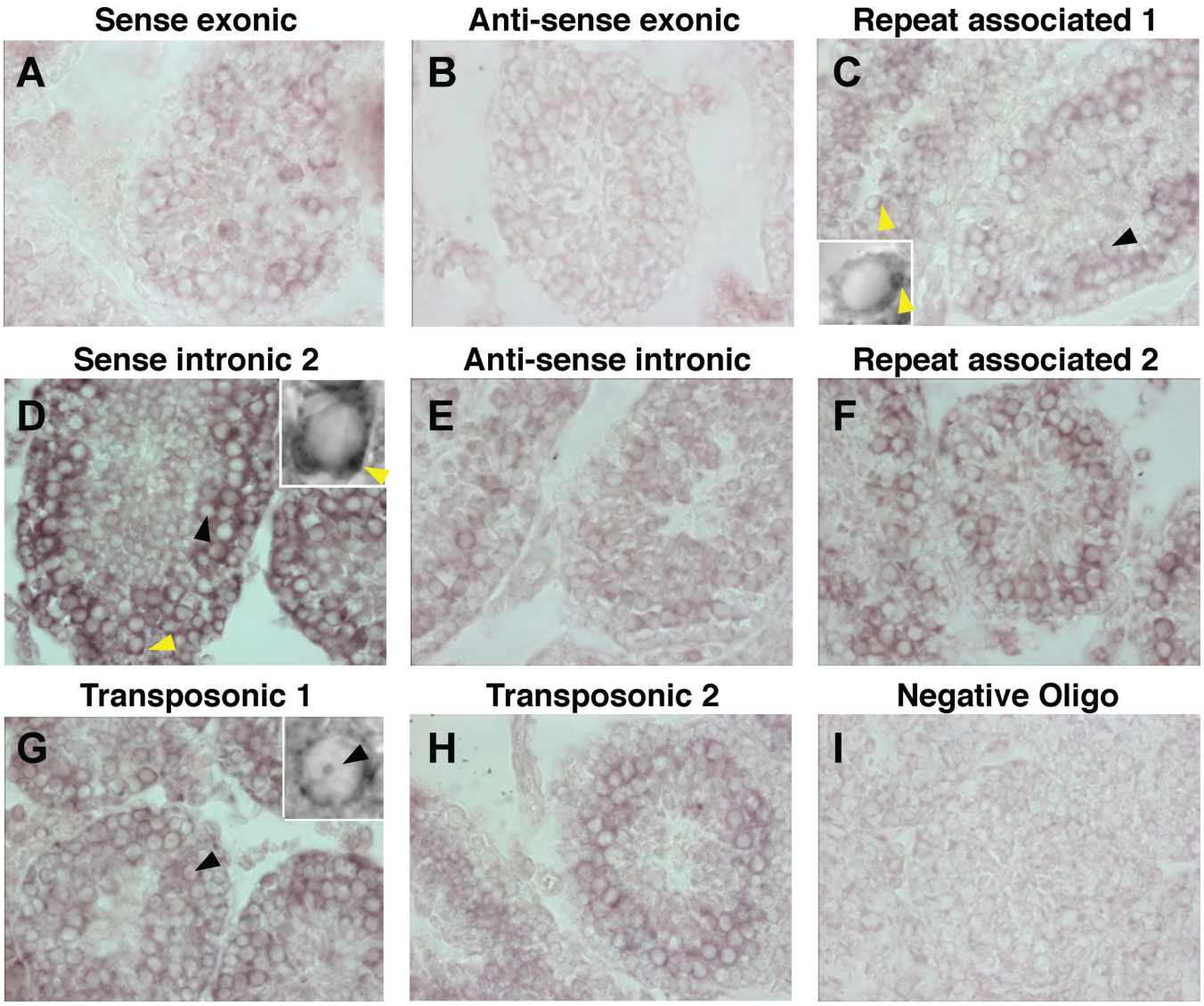

Figure 2. piRNAs are abundantly expressed in spermatocytes

In situ hybridization analysis on the adult testis shows that piRNAs are abundant in the cytoplasm of spermatocytes. In addition to the homogenous cytoplasmic staining, piRNAs localize to peri-nuclear puncta that resemble nuage/chromatoid bodies. Early spermatocytes show a nuclear punctum staining as well. Cell type assessment was based on cellular morphology and relative location to the lumen periphery. Yellow arrowhead in **C, D**, and their insets: chromatoid body-like staining; black arrowhead in **C, D**, and **G**: nuclear punctum staining. Insets are the magnified views of the regions indicated with the arrowheads. Each panel corresponds to an individual piRNA staining, described by the region it is derived from (e.g; anti-sense exonic: a piRNA derived from the anti-sense strand of an exon). The sequences for these piRNAs are listed in Materials and Methods. Negative oligo: a 28mer oligonucleotide without a match on the genome was used as the negative control to assess the background level. “Sense-intronic 2” is a MIWI piRNA, the rest are MILI piRNAs.

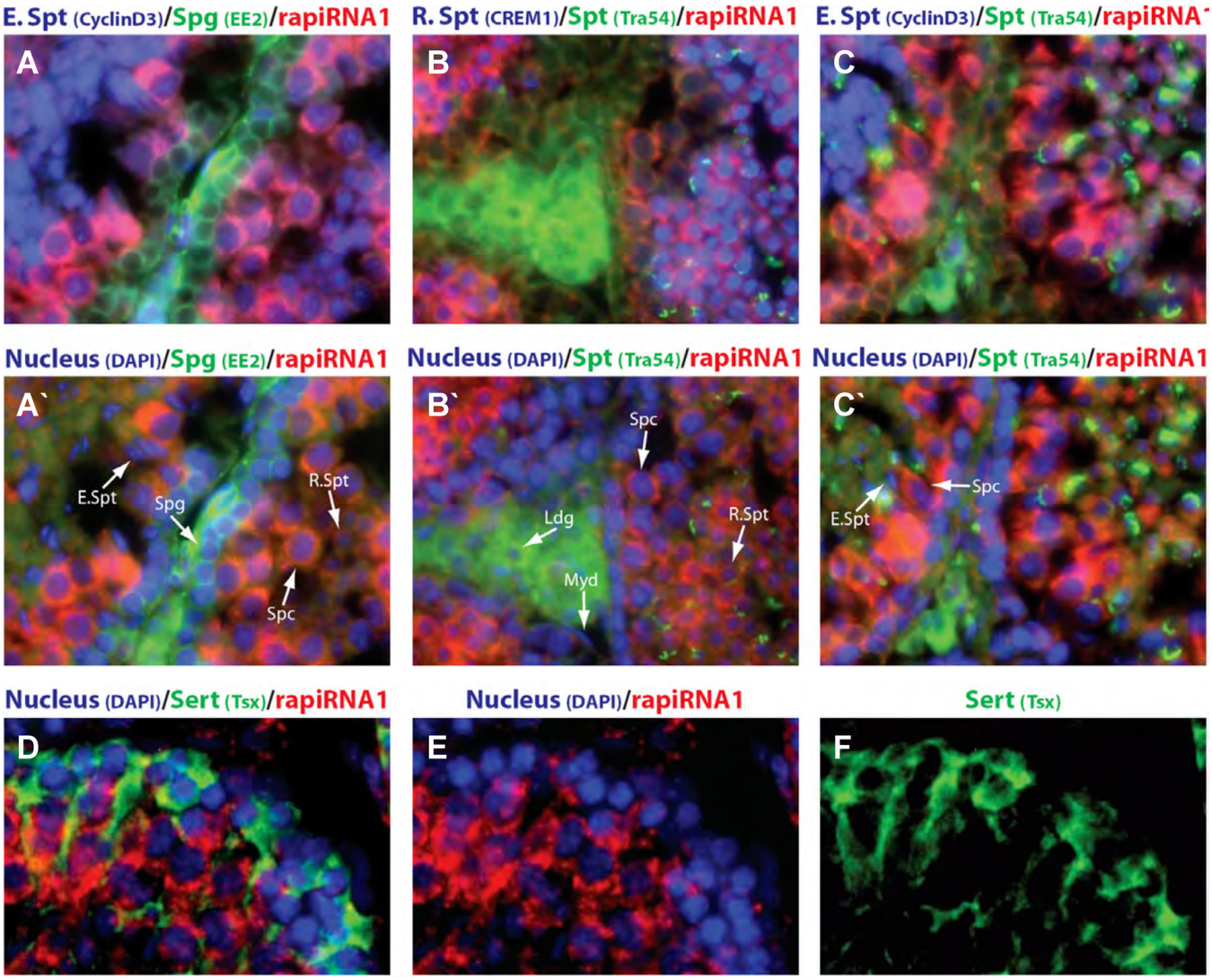

Figure 3. piRNAs are germline-specific

Co-staining for cell type-specific markers confirms the expression of the piRNA tested is highly abundant in spermatocytes (A–C, A`–C`) and moderately abundant in spermatids (B, B`) but close to the background level in spermatogonia (A, A`) and elongating spermatids (A, A`–C, C`). It is not detectable in the interstitial soma Leydig and Myeoid cells (B, B`), and luminal soma Sertoli cells (D–F). Shown are wildtype adult testis sections. Spg: Spermatogonia, Spt: Spermatid, R.Spt: Round spermatid, E.Spt: Elongating spermatid, Spc: Spermatocyte, Sert: Sertoli Cell, Ldg: Leydig cell, Myd: Myeoid cell, rapiRNA1: repeat-associated piRNA1. Shown in parentheses are the markers used. Middle panels correspond to the nuclear staining of the uppermost panels with DAPI in blue.

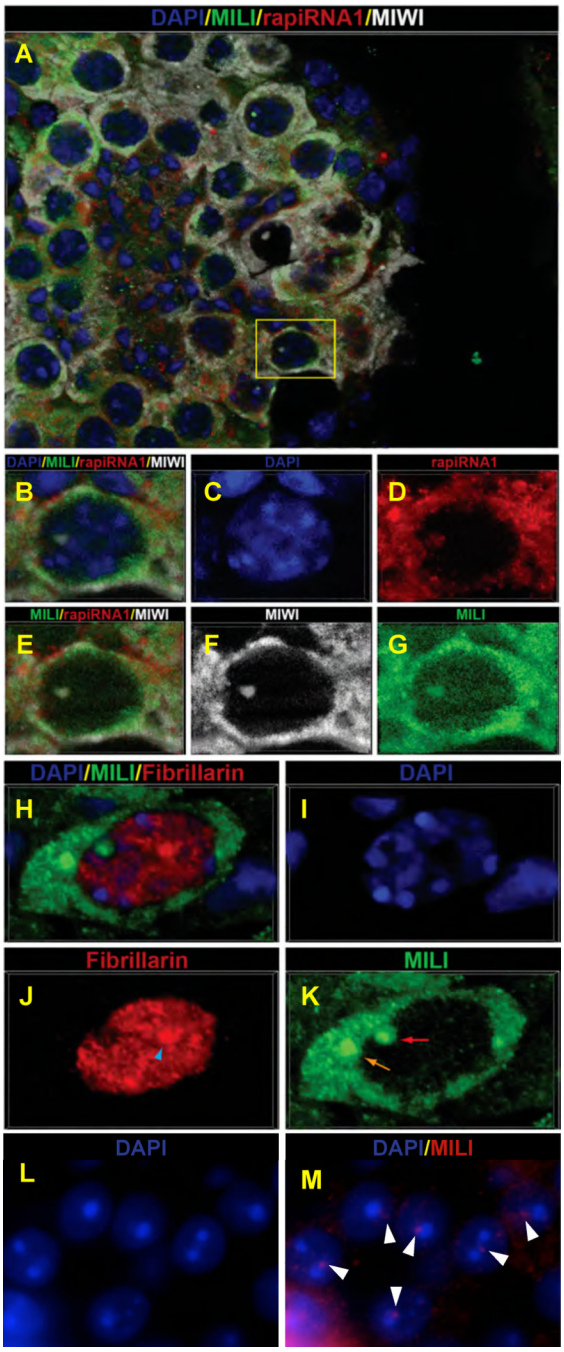

Figure 4. piRNAs, MIWI, and MILI localize to the dense body and chromatoid body

A–G. MILI, MIWI, and piRNAs localize to a DAPI-negative nuclear punctum present only in primary spermatocytes. Shown in **B–G** is the magnified view of the spermatocyte boxed in A. **H–K**. Co-staining for a nucleolus/Cajal body marker, fibrillarin, shows that the nuclear punctum is not part of nucleolus or Cajal body. L–M. An immunofluorescence micrograph of MILI (red in M) and DAPI during spermatogenesis, showing that MILI is localized to peri-chromocenter in round spermatids. Cyan arrowhead in **K**: nucleolus; orange arrow in **K**: nuage/chromatoid body-like structure; red arrow: “dense body”-like structure; white arrowheads: MILI Images are 3μm thick 3D views except that L and M are conventional

microscopic images of 10 μm sections. The immunofluorescence was performed on wildtype adult testis cryosections.

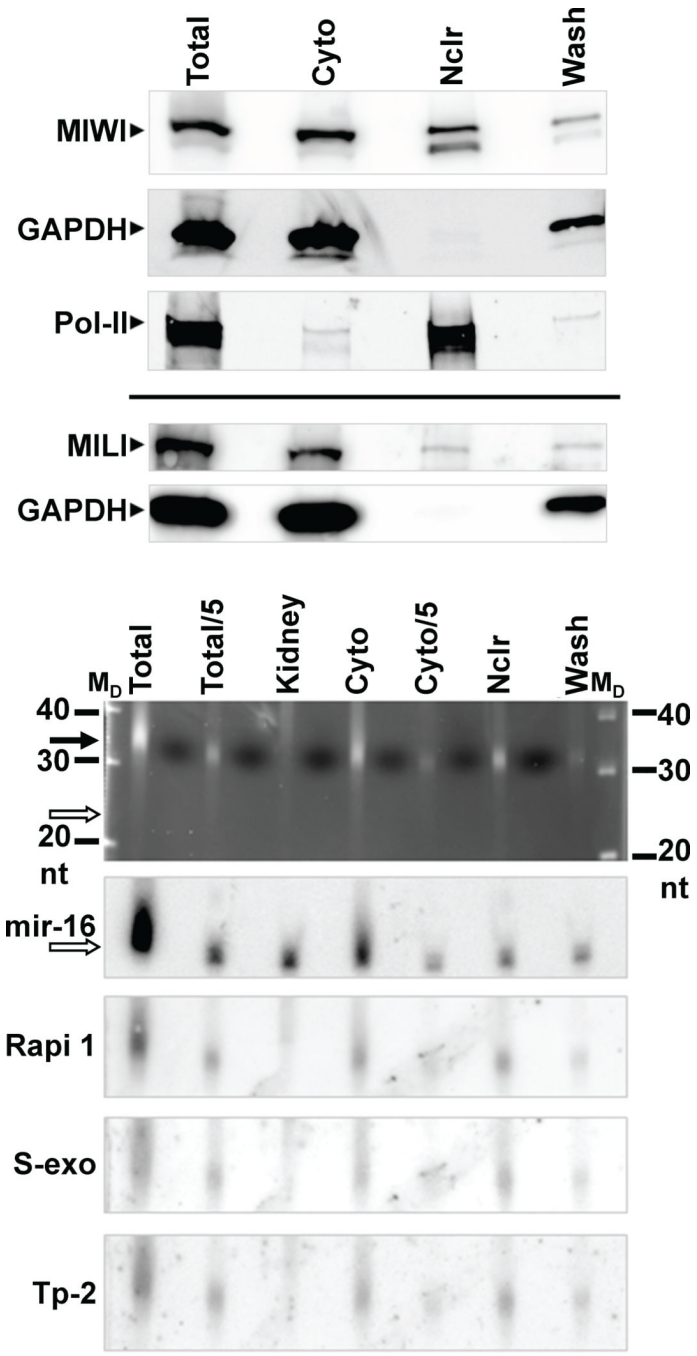

Figure 5. MILI, MIWI, and piRNAs exist in the nucleus as well as cytoplasm

A. Western blots of equal volumes of testicular fractions, showing the sub-cellular distribution of MIWI and MILI, with GAPDH and phosphoserine 5 RNA Polymerase II (Pol-II) used as cytoplasmic and nuclear markers, respectively, to assess the purity of the fractionation. Samples from the same fractions have been analyzed in two separate occasions, stripped and re-probed as required. Those analyses from different gels are separated by the horizontal bar. **B**. Northern blots of equal volumes of fractionated RNAs, showing the sub-cellular distribution of piRNAs. Ethidium bromide staining at the top panel shows total piRNA population in each sample; whereas the four northern blots show the

level of individual piRNAs. 25 μg total RNA from kidney was used as a negative control, where microRNA miR-16, but not piRNAs, is detected. Total: Unfractionated testicular extract; cyto: Cytoplasmic fraction; Nclr: Nuclear fraction. M_D: 10nt DNA marker, S-exo: Sense exonic, Tp2: Transposonic 2, Rapi1: Repeat-associated 1. Blank arrow indicates the location of mir-16.

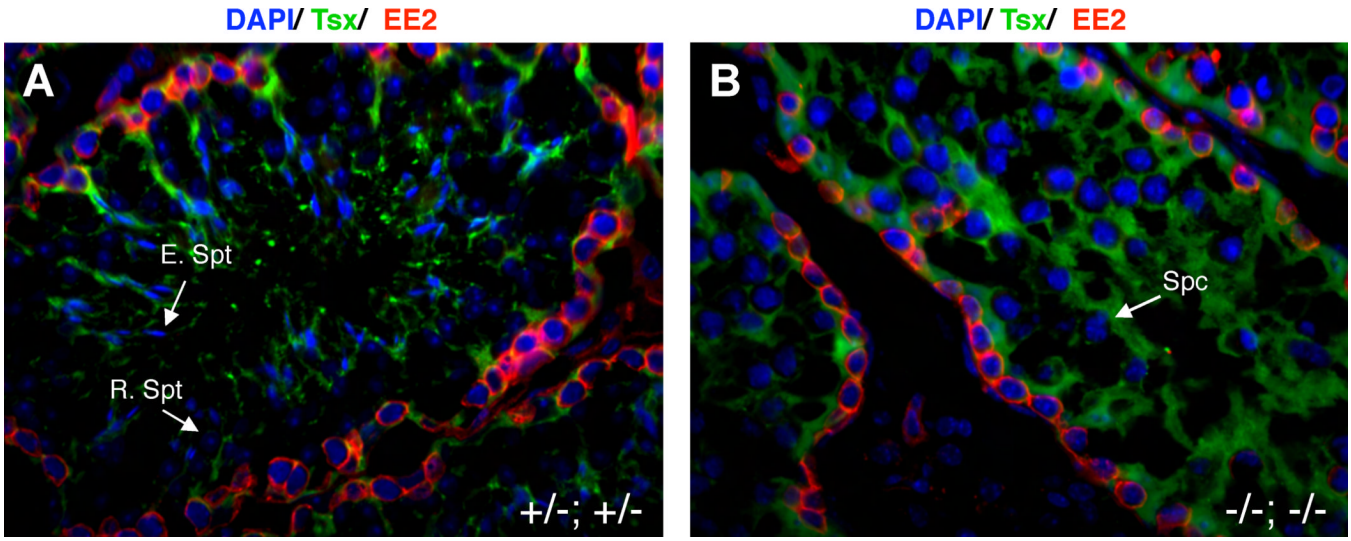

Figure 6. Spermatogenesis is arrested during meiosis in *Miwi*$^{-/-}$; *Mili*$^{-/-}$ mice

A. *Miwi*$^{+/-}$; *Mili*$^{+/-}$ (+/−; +/−) testes show the full complement of germ cells. **B**. *Miwi*$^{-/-}$; *Mili*$^{-/-}$ (−/−; −/−) testes do not consist of germ cells beyond primary spermatocyte stage. Germ cell types are assessed based on DAPI staining and the spermatogonia marker EE2. Tsx was used to mark Sertoli cells. The histological analysis was performed on testis cryosections of 14 weeks old mice. R.Spt: Round spermatid, E.Spt: Elongating spermatid, Spc: Primary spermatocyte.

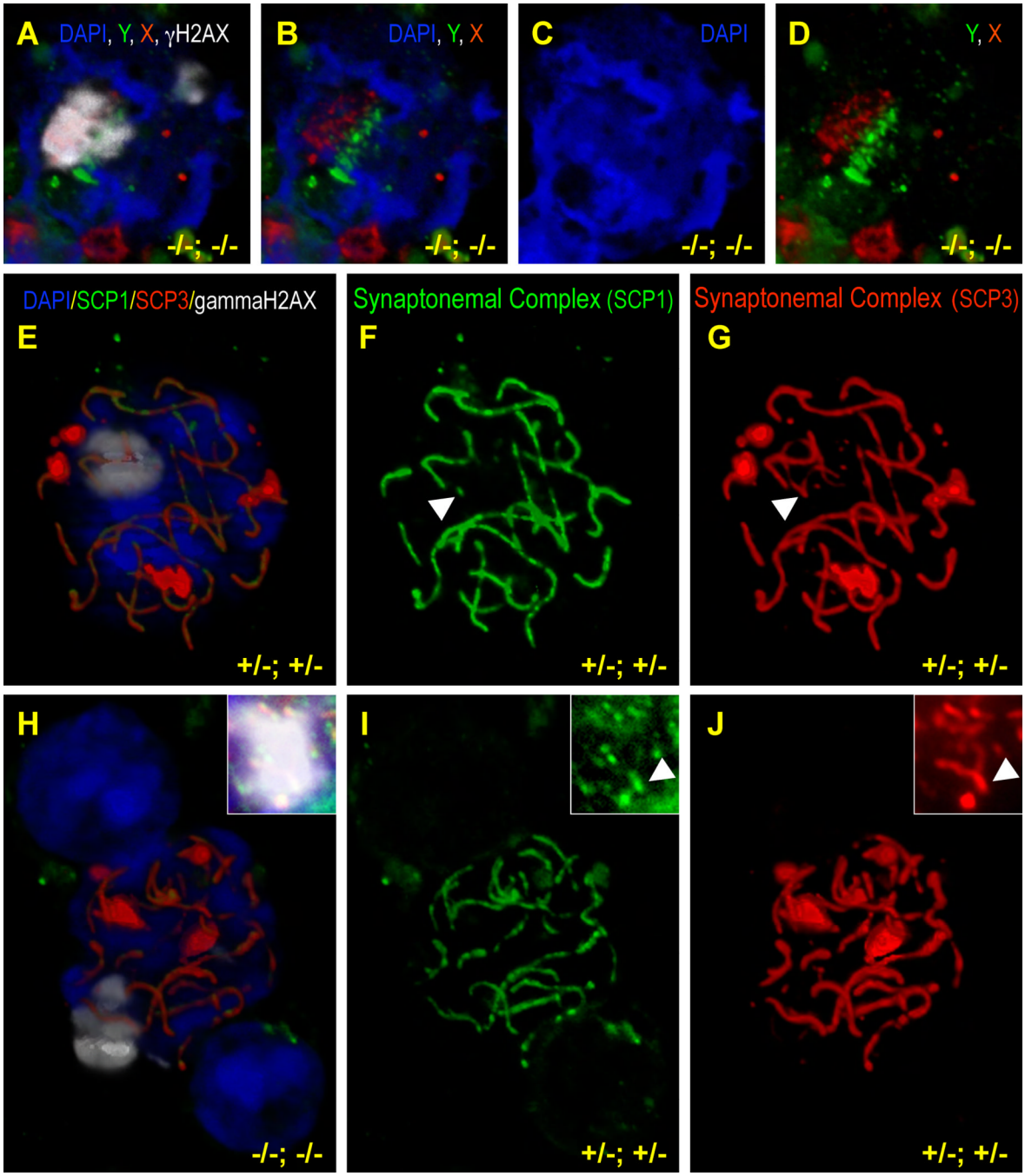

Figure 7. *Miwi*$^{-/-}$; *Mili*$^{-/-}$ spermatocytes are not defective in synapsis of homologous chromosomes

A–D. Co-staining of spermatocyte spreads from 6 weeks old *Miwi*$^{-/-}$*Mili*$^{-/-}$ (−/−; −/−) mice for DNA (DAPI), X and Y chromosomes and the sex-body (γH2AX) shows that the sex chromosomes of *Miwi*$^{-/-}$; *Mili*$^{-/-}$ spermatocytes are able to recognize each other during homologous chromosome pairing in meiosis, and can aggregate into a compact XY body. Shown is a 2-μm 3D image of a pachytene spermatocyte identified by the globular γH2AX staining over the sex chromosomes. **E–J**. Co-staining of spermatocyte spreads from six-week old *Miwi*$^{+/-}$; *Mili*$^{+/-}$ (+/−; +/−) mice (**E–G**) and *Miwi*$^{-/-}$; *Mili*$^{-/-}$ mice (−/−; −/−) (**H–J**) for the transverse (SCP1) and lateral (SCP3) elements of the synaptonemal complex

shows that synapsis in *Miwi*$^{-/-}$; *Mili*$^{-/-}$ testes is not overtly impaired. DAPI and γH2AX were used to stain DNA and the XY body, respectively. White arrowheads point the synapsed pseudo-autosomal regions of the sex chromosomes. Shown are 5–7μm 3D images of pachytene stage spermatocytes. Insets are the 2D images of the XY body in a different *Miwi*$^{-/-}$; *Mili*$^{-/-}$ spermatocyte sample.

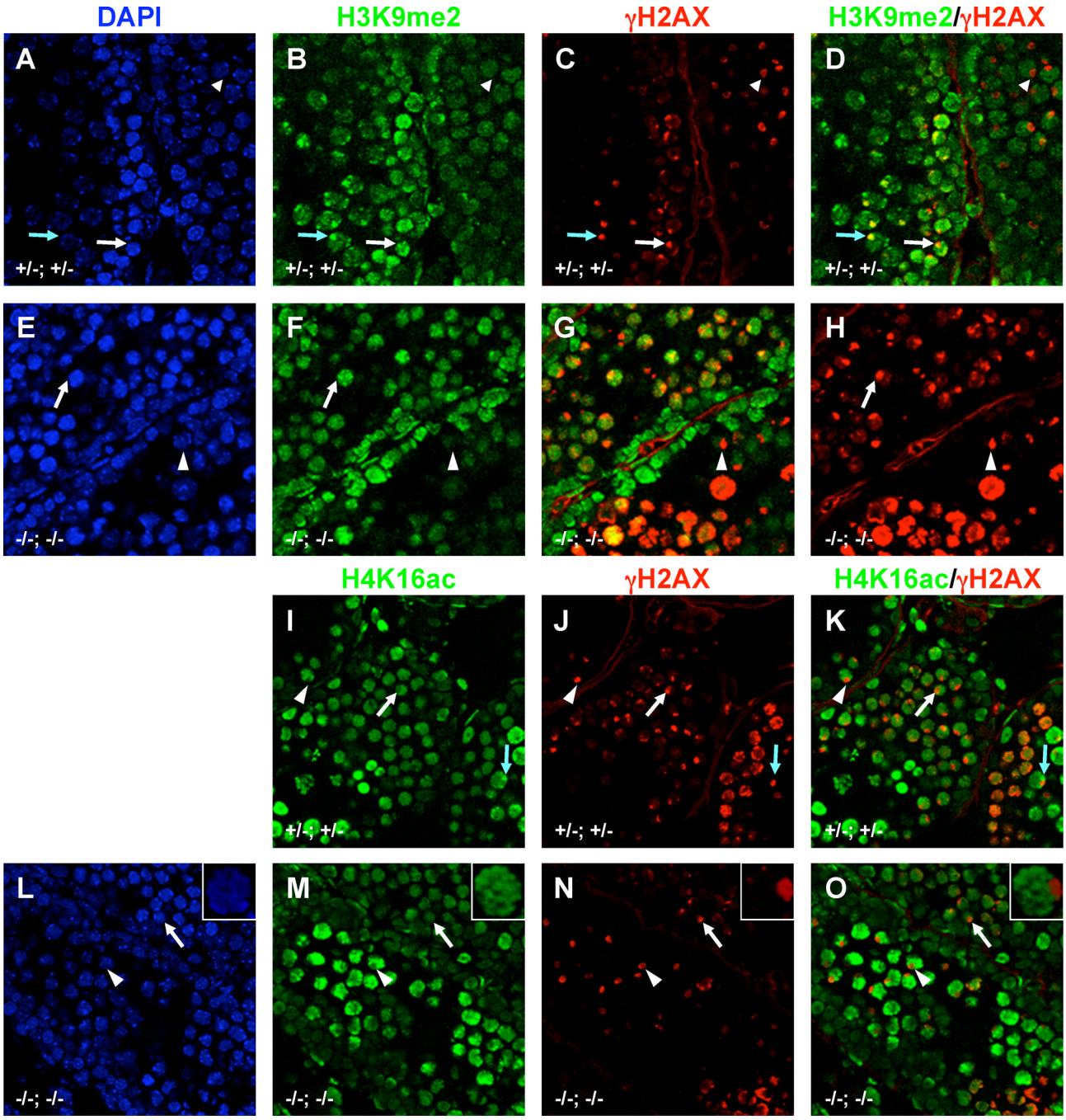

Figure 8. *Miwi*$^{-/-}$*; Mili*$^{-/-}$ spermatocytes are arrested when the XY body undergoes epigenetic changes

Co-staining of 18-dpp *Miwi*$^{+/-}$*; Mili*$^{+/-}$ (+/−; +/− in **A–D** and **I–K**) and *Miwi*$^{-/-}$*;Mili*$^{-/-}$ (−/−; −/− in **E–H and L–O**) testis cryosections for DNA (DAPI) (**A, E, L**), γH2AX (**C–D, G–H, J–K, N–O**) and the heterochromatin mark H3K9me2 (**B, D, F, H**) or euchromatic mark H4K16ac (**I, K, M, O**) shows that *Miwi*$^{-/-}$*; Mili*$^{-/-}$ spermatocytes are arrested before the XY body is enriched with H3K9me2 but after it is depleted of H4K16ac. White and blue arrows point to the examples of the XY bodies (globular γH2AX) in early and late pachytene spermatocytes respectively, while white arrowheads point to those in mid-pachytene spermatocytes. No germ cell beyond midpachynema is observed in *Miwi*$^{-/-}$*;*

Mili$^{-/-}$ testes. Insets in L-O show an example of early pachytene spermatocyte that displays a euchromatin XY body in a 14 weeks old *Miwi*$^{-/-}$*; Mili*$^{-/-}$ mouse.

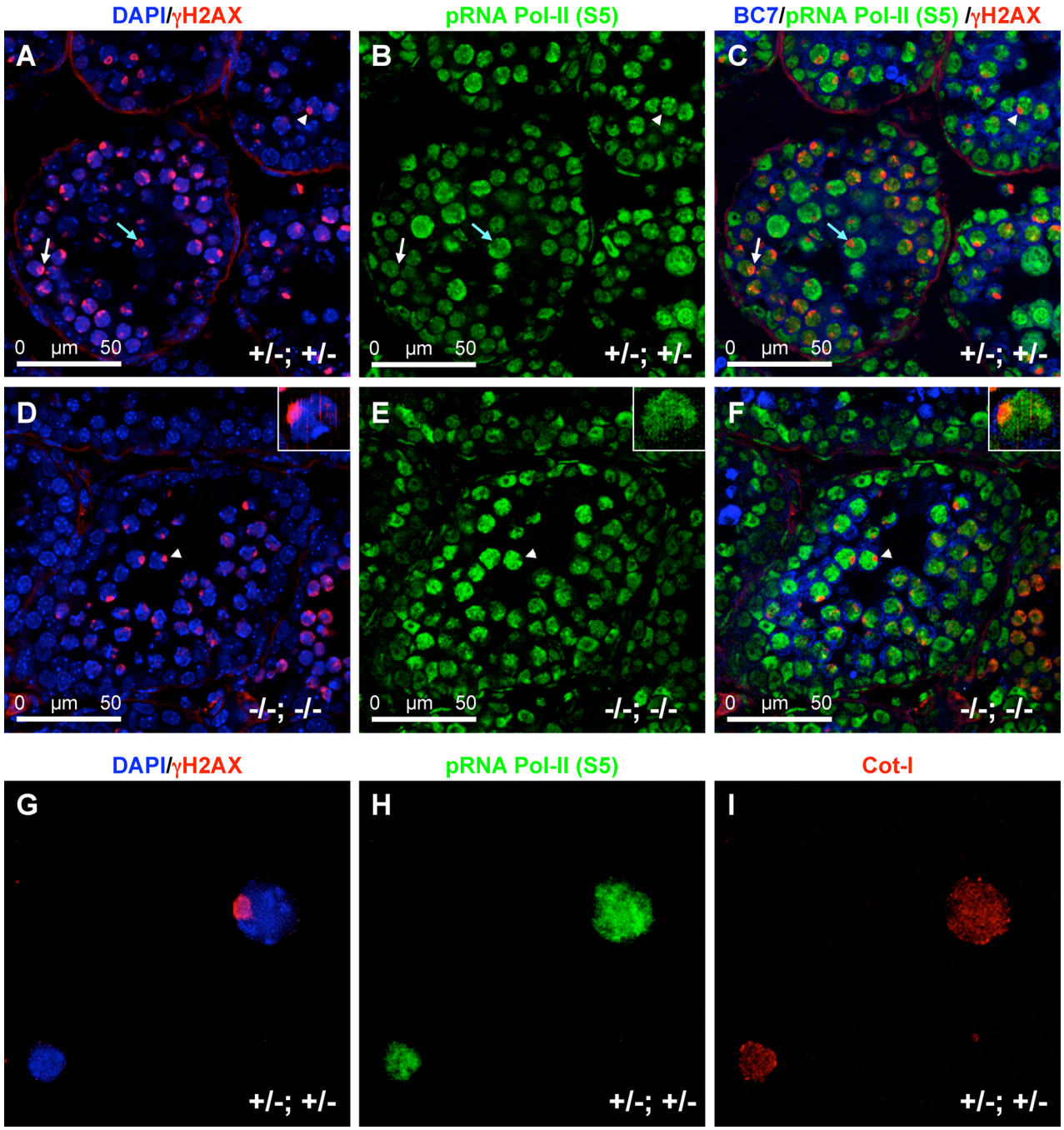

Figure 9. The XY body in *Miwi*$^{-/-}$; *Mili*$^{-/-}$ spermatocytes still undergoes transcriptional silencing

A–F: Co-staining of 18 dpp *Miwi*$^{+/-}$; *Mili*$^{+/-}$ (+/−; +/−) (**A–C**) and *Miwi*$^{-/-}$; *Mili*$^{-/-}$ (−/−; −/−) (**D–F**) testicular cryosections for DAPI (**A, D**), γH2AX (**A, C, D, F**), a zygotene and pachytene spermatocyte marker BC7 (**C, F**), and Ser5-phosphorylated RNA polymerase II (pRNA polII-S5) (**B, C, E, F**) shows that the XY body in *Miwi*$^{-/-}$; *Mili*$^{-/-}$ spermatocytes still undergoes progressive depletion for the activated form of RNA polymerase II. White and blue arrows point to the examples of the XY bodies (globular γH2AX) in early and late pachytene spermatocytes respectively, while white arrowheads point to those in mid-pachytene spermatocytes. No germ cell beyond mid-pachynema is observed in *Miwi*$^{-/-}$;

Mili$^{-/-}$ testis. Insets in D–F show an example of *Miwi*$^{-/-}$*; Mili*$^{-/-}$ early pachytene spermatocyte, which still largely displays pPolII-S5 signal on the XY body as its stage-matched *Miwi*$^{+/-}$*; Mili*$^{+/-}$ counterpart (white arrow in A–C). **G–I**: Staining of 18dpp *Miwi*$^{+/-}$*; Mili*$^{+/-}$ spermatocyte spreads for Cot-1 RNA, which represents the nascent transcripts, recapitulates the lack of pRNA-PolII-S5 on the XY body.